Hydrol. Earth Syst. Sci. Discuss., 12, 8175–8220, 2015
www.hydrol-earth-syst-sci-discuss.net/12/8175/2015/
doi:10.5194/hessd-12-8175-2015

Hydrology and Earth System Sciences Discussions
Open Access

On the propagation of diel signals in river networks using analytic solutions of flow equations

M. Fonley[1,2,4], **R. Mantilla**[2,3], **S. J. Small**[2], **and R. Curtu**[1]

[1]Department of Mathematics, University of Iowa, Iowa City, Iowa, USA
[2]Iowa Flood Center, IIHR Hydroscience and Engineering, University of Iowa, Iowa City, Iowa, USA
[3]Department of Civil and Environmental Engineering, University of Iowa, Iowa City, Iowa, USA
[4]Department of Mathematics, Alma College, Alma, Michigan, USA

Received: 4 August 2015 – Accepted: 5 August 2015 – Published: 24 August 2015

Correspondence to: M. Fonley (fonleymr@alma.edu)

Published by Copernicus Publications on behalf of the European Geosciences Union.

Abstract

Two hypotheses have been put forth to explain the magnitude and timing of diel streamflow oscillations during low flow conditions. The first suggests that delays between the peaks and troughs of streamflow and daily evapotranspiration are due to processes occurring in the soil as water moves toward the channels in the river network. The second posits that they are due to the propagation of the signal through the channels as water makes its way to the outlet of the basin. In this paper, we design and implement a theoretical experiment to test these hypotheses. We impose a baseflow signal entering the river network and use a linear transport equation to represent flow along the network. We develop analytic streamflow solutions for two cases: uniform and nonuniform velocities in space over all river links. We then use our analytic solutions to simulate streamflows along a self-similar river network for different flow velocities. Our results show that the amplitude and time delay of the streamflow solution are heavily influenced by transport in the river network. Moreover, our equations show that the geomorphology and topology of the river network play important roles in determining how amplitude and signal delay are reflected in streamflow signals. Finally, our results are consistent with empirical observations that delays are more significant as low flow decreases.

1 Introduction

Many authors have observed daily fluctuations in streamflow during periods of little or no rain (e.g., Bond et al., 2002; Graham et al., 2013; Gribovszki et al., 2008; Wondzell et al., 2007). These fluctuations have been attributed to various causes, especially to those driven by temperature, which undergo a daily cycle. Temperature affects several hydrological processes, including freeze/thaw rates, evaporation rates, viscosity of water, and transpiration rates. Although many factors may contribute to the daily cycle of streamflow, evapotranspiration seems to be dominant (Gribovszki et al., 2010). Hydro-

HESSD
12, 8175–8220, 2015

logic processes during periods of low flow are often overlooked in favor of investigating high flow and subsequent flood conditions. In spite of this, the consequences of hydrological processes during low flow remain critical in dictating land use and agricultural types (Mul et al., 2011), indicating the extent of global climate change (Arnell, 1998), and influencing the chemical makeup of water downstream (Stott and Burt, 1997) or the availability of water, which impacts fish populations and water treatment requirements (Burn et al., 2008).

Graham et al. (2013) have compiled a collection of suggested explanations for the behavior of oscillatory streamflow under dry conditions, including several hypotheses that suggest that water moves differently through the subsurface as the hillslope drains. On the other hand, the authors of Wondzell et al. (2007) suggest that streamflow properties are the result of attenuation as flow propagates along the river link with decreasing velocity, which causes the flow to be increasingly "out of phase". During dry periods of low flow, the time between the maximum evapotranspiration and the minimum streamflow values has been of particular interest because this time delay grows as the dry season progresses, indicating that the response of the streamflow to the evapotranspiration forcing on water in the hillslope slows as more water is removed from the system.

In this paper, we aim to design and implement an analytic experiment to test these hypotheses through a theoretical approach. We start by assuming a particular baseflow pattern in each river link of a given river network (e.g., fluctuations with exponentially decaying amplitude). Thus, the selected pattern exhibits attributes of observed baseflow. Then, we work with simplified modeling conditions such as the linear transport equation to develop an analytic solution for the flow at any given point along the river network. By fixing the baseflow pattern, we remove the dependence of streamflow properties (e.g., amplitude and time delay) on soil processes. If the resulting streamflows along the river network exhibit oscillations with different time delays and amplitudes, then we conclude that the effects described in Wondzell et al. (2007) can be induced by different velocities in a river network, even in the absence of changes induced by groundwater processes. Importantly, our theoretical results include algorithmic calculations of the phase shifts caused by the river network and their relationship to stream velocity. The latter can be used to make predictions about streamflow at any point in the river network, in particular with respect to the time delay between maximum evapotranspiration and minimum streamflow.

The paper is structured in the following way: in Sect. 2, we consider a certain baseflow pattern and a linear transport equation to represent flow along the river network. In Sect. 2.1.1, we compute an analytic solution for the partial streamflow at the outlet of a river network due to baseflow applied to one upstream hillslope. Then, in Sect. 2.1.2, we assemble the complete solution at the outlet when all hillslopes in the network experience the same baseflow and all links in the network have uniform properties. We then describe the general case of nonuniform river networks in Sect. 2.2. Section 3.2 through Sect. 3.4 describe our experiment to test the effects of river network velocity on streamflow attributes and support the claim that decreasing amplitude and increasing time delay in the streamflow at the network outlet can be attributed to delays in the river network. Finally, Sect. 4 contains a short concluding discussion and ideas for future work.

2 Developing an analytic solution for streamflow based on river network geometry

Let us now assume that the total runoff from each hillslope into a river link in a given river basin is oscillatory and its amplitude undergoes exponential decay (as seen for baseflow under dry conditions). Then, we define the runoff by the formula

$$R(t) = Be^{-At} + Ce^{-At}\sin(2\pi \nu t), \quad (1)$$

with A, B, C, and ν positive parameters and $C < B$ to ensure that the baseflow takes only positive values. In this paper, we apply the same baseflow pattern to all hillslopes on the river network beginning everywhere at an initial time $t = 0$ (see the left panel

HESSD
12, 8175–8220, 2015

of Fig. 1). Note that in this setup, the runoff oscillations are supposed to be driven by evapotranspiration, which is synchronized over all hillslopes at the catchment scale. For this reason, synchronized timing of the forcing seems an acceptable hypothesis.

A sample baseflow pattern with parameter values $A = 0.003$ [$\mathrm{h^{-1}}$], $B = 0.08$ [$\mathrm{L\,s^{-1}}$], $C = 0.008$ [$\mathrm{L\,s^{-1}}$], and $v = \frac{1}{24}$ [$\mathrm{h^{-1}}$] is illustrated in the right panel of Fig. 1. We chose the value of v so that the frequency of the oscillations corresponds to a period of 24 hours, representing a diurnal signal. If we assume that the baseflow is linearly related to the amount of water in the soil, then A corresponds to the linear rate of water movement through the soil.

In this paper, the streamflow at the outlet of a river link is defined by the transport equation, which has been derived from the conservation of mass in the associated river link

$$\frac{\mathrm{d}q_i(t)}{\mathrm{d}t} = K(q_i)(R(t) + q_{i1}(t) + q_{i2}(t) - q_i(t)). \qquad (2)$$

The input to the link comes from runoff in adjacent hillslopes and from the streamflow of upstream tributary links. Therefore, the only method for water to exit the link is as streamflow at the link outlet. Here, q_{i1} and q_{i2} are the flows from the upstream tributary links. If a link i has more than two tributaries at its upstream node, more terms can be added in Eq. (2), accordingly. For our calculation, we assume the function $K(q_i)$ to be constant, $K(q_i) = v_i/l$, where v_i is the velocity of link i and l is the length of the link, which is assumed to be uniform over all links in the network (Mantilla et al., 2011). For simplicity, $K(q_i)$ will be called k_i.

To determine the streamflow at the river network outlet, we first consider the influence of runoff on a single hillslope and how that runoff signal propagates downstream; see Sect. 2.1.1 and Fig. 2. Then, in Sect. 2.1.2, we will assemble the information derived for all links of the river network into one comprehensive solution by applying the superposition principle. Until this point, our calculations will cover only the case involving uniform conditions on the links in the river network (assuming that all links share a velocity and the same transport constant k). In Sect. 2.2 we generalize the solution for the construction of the analytic formulation for the nonuniform case (assuming different values of k_i for each link i in the network).

2.1 Uniform velocity

In the case of uniform velocities over the river network, the transport constant, k_i, is subsequently the same for all links in the network. In this subsection, it will be called k.

2.1.1 Hillslope runoff signal propagation on river networks with uniform velocity

As mentioned above, we first apply runoff $R(t)$ to a given hillslope, denoted as "hillslope a", with adjacent river link 1. Because the transport equation for each link is linear, we can independently trace the runoff entering link 1 as it flows through the river network and then use superposition to combine the flows entering each river link. This would not be possible if the transport equation contained a nonlinear component.

When the runoff entering link 1 has gone through *one* river link only ("Step 1" see Fig. 2), the flow q_1 at the outlet of link 1 is the solution to the differential equation

$$\frac{\mathrm{d}q_1(t)}{\mathrm{d}t} = k(Be^{-At} + Ce^{-At}\sin(2\pi\nu t) - q_1(t)). \tag{3}$$

That is

$$q_1 = (q_1(0) - \mathcal{J}_1 + \mathcal{K}_1\sin(2\pi\nu\theta))\,e^{-kt} + (\mathcal{J}_1 + \mathcal{K}_1\sin(2\pi\nu(t-\theta)))\,e^{-At}, \tag{4}$$

with $q_1(0)$ the initial condition (at $t=0$) of the flow in link 1, and $\mathcal{K}_1$, $\mathcal{J}_1$, and θ defined by

$$\mathcal{K}_1 = \frac{Ck}{\sqrt{(k-A)^2 + 4\pi^2\nu^2}}$$

$$\mathcal{J}_1 = \frac{Bk}{k-A} \tag{5}$$

HESSD
12, 8175–8220, 2015
On the propagation of diel signals in river networks using analytic solutions
M. Fonley et al.

and

$$\sin(2\pi\nu\theta) = \frac{2\pi\nu}{\sqrt{(k-A)^2 + 4\pi^2\nu^2}}$$
$$\cos(2\pi\nu\theta) = \frac{k-A}{\sqrt{(k-A)^2 + 4\pi^2\nu^2}}. \tag{6}$$

Note that $\theta \in (0, \frac{1}{4\nu})$ is the resulting time delay for the fluctuating pattern $q_1(t)$ of frequency ν compared to the input signal $R(t)$.

At Step 2, when the runoff has traversed *two* river links, we need to compute $q_2(t)$ by taking into account the solution $q_1(t)$ from Step 1 (see Fig. 2, second panel). Since we assumed for the moment that $q_1(t)$ has been transmitted downstream via the next link (link 2), with no additional runoff, the streamflow at the end of link 2 is given by

$$q_2 = [(q_2(0) - \mathcal{J}_2 + \mathcal{K}_2 \sin(2\pi\nu\theta_2)) + kt\,(q_1(0) - \mathcal{J}_1 + \mathcal{K}_1 \sin(2\pi\nu\theta_1))]\, e^{-kt}$$
$$+ (\mathcal{J}_2 + \mathcal{K}_2 \sin(2\pi\nu(t-\theta_2)))\, e^{-At}$$

with $\theta_1 = \theta$, $\theta_2 = 2\theta$, and

$$\mathcal{K}_2 = \frac{Ck^2}{(k-A)^2 + 4\pi^2\nu^2}$$
$$\mathcal{J}_2 = \frac{Bk^2}{(k-A)^2}.$$

By mathematical induction, we then compute the solution $q_n(t)$, $n \geq 1$ of flow measured downstream at the exit from link n. This takes the form:

$$q_n(t) = e^{-At}\,[\mathcal{J}_n + \mathcal{K}_n \sin(2\pi\nu(t-\theta_n))] + e^{-kt} \sum_{j=0}^{n-1} \mathcal{L}_{n-j} \frac{(kt)^j}{j!} \tag{7}$$

HESSD
12, 8175–8220, 2015

On the propagation of diel signals in river networks using analytic solutions

M. Fonley et al.

with coefficients

$$\mathcal{K}_n = C\prod_{j=1}^{n}\frac{k}{\sqrt{(k-A)^2+4\pi^2\nu^2}} = C\left(\frac{k}{\sqrt{(k-A)^2+4\pi^2\nu^2}}\right)^n, \qquad n \geq 1$$

$$\mathcal{J}_n = B\prod_{j=1}^{n}\frac{k}{k-A} = B\left(\frac{k}{k-A}\right)^n, \qquad n \geq 1 \tag{8}$$

$$\theta_n = \sum_{i=1}^{n}\theta = n\theta, \qquad n \geq 1$$

and

$$\mathcal{L}_j = q_j(0) - \mathcal{J}_j + \mathcal{K}_j \sin\left(2\pi\nu\theta_j\right), \quad j = 1, 2, \ldots n. \tag{9}$$

Here, $q_j(0)$ represents the initial condition for the flow in link j. For clarity, we included the details of this algorithmic proof in Appendix A.

2.1.2 Assembling the complete solution for streamflow at the outlet

The goal of this section is to determine the equation for the streamflow at a given point of calculation along the river network, in particular at the network outlet. We take the parameters representing properties of each river link to be uniform over all links in the network (i.e., same parameter k) so that the influence of two links that are equidistant (topologically speaking) from the outlet will be the same. The solution determined in Sect. 2.1.1, however, shows only the *partial contribution* of link i to the streamflow, as it propagates downstream without considering any additional runoff. Therefore, in order to determine the *complete* streamflow solution, one must sum the overall contributions from runoff on each upstream link. This can be done if the topological representation of the river network is known or if the topological width function upstream of the outlet is used. The width function for a given link i and distance n (denoted $W_n^{(i)}$) is an integer representing the number of river links of topological distance n upstream of link i, where $W_1^{(i)} = 1$ and corresponds to link i itself. For a fixed location in the river network, the width function can be written as a vector whose length is the diameter (i.e., the longest path) upstream of link i. The network depicted in Fig. 3 further illustrates this process.

First, we will focus on the outlet of link a (before the streamflow from a combines with that of link b); see Fig. 3. We recognize one link upstream of this point: link a. Then, the only contribution to the streamflow at this point is from the runoff to link a that has traversed *one* link. The width function at this point has only one element and there is only one link of distance 1, so the width function, a 1-dimensional vector, is given by $W^{(a)} = [1]$, and the streamflow is simply

$$q_a = 1 \times q_1 = q_1 = \mathcal{L}_1 e^{-kt} + e^{-At}[\mathcal{J}_1 + \mathcal{K}_1 \sin(2\pi\nu(t - \theta_1))]. \tag{10}$$

On the other hand, if we compute streamflow at the outlet of link e (prior to joining link f; see Fig. 3), we have one link of topological distance 1 (link e) and two links of topological distance 2 (links a and b). Then, the width function is given by the vector $W^{(e)} = [1\ 2]$. This means that the runoff from link e has only traversed one link to get to the outlet, but the runoff from either of the links a or b has traversed two links. The total flow at the outlet of link e is

$$q_e = 1 \times q_1 + 2 \times q_2 = q_1 + 2q_2. \tag{11}$$

After applying the formulas for q_1 and q_2, similar terms can be collected in the following way

$$\begin{aligned} q_e &= \mathcal{L}_1 e^{-kt} + e^{-At}[\mathcal{J}_1 + \mathcal{K}_1 \sin(2\pi\nu(t - \theta_1))] \\ &\quad + 2[\mathcal{L}_2 + kt\mathcal{L}_1]e^{-kt} + 2[\mathcal{J}_2 + \mathcal{K}_2 \sin(2\pi\nu(t - \theta_2))]e^{-At} \\ &= e^{-At}(\mathcal{J}_1 + 2\mathcal{J}_2 + \mathcal{K}_1 \sin(2\pi\nu(t - \theta_1)) + 2\mathcal{K}_2 \sin(2\pi\nu(t - \theta_2))) \\ &\quad + e^{-kt}(\mathcal{L}_1 + 2[\mathcal{L}_2 + kt\mathcal{L}_1]). \end{aligned} \tag{12}$$

HESSD
12, 8175–8220, 2015

To complete this example, let us now consider the width function at the outlet of the network in Fig. 3, which is $W^{(i)} = [1\ 2\ 2\ 4]$. The first element of $W^{(i)}$ corresponds to link i; the second element ($W_2^{(i)} = 2$) corresponds to links g and h; the third element ($W_3^{(i)} = 2$) corresponds to links e and f; and the last component ($W_4^{(i)} = 4$) corresponds to links a–d. The diameter of this network is $D_i = \text{length}(W^{(i)}) = 4$. Note that the total number of links in the network is also the sum of the elements of the width function, since each link has a corresponding distance from the outlet. For this, we can use the notation: $|W^{(i)}| = \sum_{n=1}^{D_i} W_n^{(i)} = 9$. For more details about the width function, see Mantilla et al. (2011). The flow at the outlet of link i is

$$q_i = 1 \times q_1 + 2 \times q_2 + 2 \times q_3 + 4 \times q_4 = \sum_{n=1}^{D_i} W_n^{(i)} q_n. \tag{13}$$

$$\begin{aligned}
&= e^{-At}\left(\mathcal{J}_1 + 2\mathcal{J}_2 + 2\mathcal{J}_3 + 4\mathcal{J}_4\right) \\
&+ e^{-At}\left(\mathcal{K}_1 \sin(2\pi\nu(t-\theta_1)) + 2\mathcal{K}_2 \sin(2\pi\nu(t-\theta_2)) + 2\mathcal{K}_3 \sin(2\pi\nu(t-\theta_3)\right. \\
&+ \left. 4\mathcal{K}_4 \sin(2\pi\nu(t-\theta_4))\right) \\
&+ e^{-kt}\left(\mathcal{L}_1 + 2[\mathcal{L}_2 + kt\mathcal{L}_1]\right. \\
&+ \left. 2\left[\mathcal{L}_3 + kt\mathcal{L}_2 + \frac{(kt)^2\mathcal{L}_1}{2!}\right] + 4\left[\mathcal{L}_4 + kt\mathcal{L}_3 + \frac{(kt)^2\mathcal{L}_2}{2!} + \frac{(kt)^3\mathcal{L}_1}{3!}\right]\right).
\end{aligned} \tag{14}$$

For a general network whose width function is given by $W^{(i)}$, the solution can be rearranged as in Eqs. (12) and (14) to get the complete solution for streamflow at the outlet i. Assuming that D_i is the diameter of the network upstream of link i, the solution at the outlet i is:

$$q_i = e^{-At} \sum_{n=1}^{D_i} W_n^{(i)} [\mathcal{J}_n + \mathcal{K}_n \sin(2\pi\nu(t-\theta_n))] + e^{-kt} \sum_{n=1}^{D_i} W_n^{(i)} \sum_{j=0}^{n-1} \mathcal{L}_{n-j} \frac{(kt)^j}{j!}. \tag{15}$$

HESSD
12, 8175–8220, 2015

The first term in Eq. (15) represents the propagation of the runoff signal from each hillslope while the second term is a result of the initial conditions coming from runoff and flow in the network. This distinction is evidenced by the rate of decay of either exponential function. The first term has a rate of decay depending upon A, and represents the decay of runoff entering the channel. The second term, conversely, has a decay rate dependent only upon k, which describes the rate of water movement through each river link.

To thoroughly interpret the components of Eq. (15), we again contemplate the physical processes being represented and use the expected parameter values to discuss the mathematical solution. First, k and A are both positive because they represent rates of water movement along the river link and through the soil, respectively. Since water will move much more quickly along the river link, which offers less resistance than soil, A is significantly less than k, so that $\frac{k}{k-A}$ has a value slightly greater than 1. Then, $\mathcal{J}_j > B$ for any value of j. Furthermore, the value of $2\pi\nu$ is fixed and is typically greater than k, which means that $\frac{k}{\sqrt{(k-A)^2+4\pi^2\nu^2}} < 1$ so that $\mathcal{K}_j < C$ for all j. This means that each component $[\mathcal{J}_n + \mathcal{K}_n \sin(2\pi\nu(t-\theta_n))]$ of the solution at the outlet shows a decrease in the amplitude of the fluctuations ($\mathcal{K}_n < C$) while increasing its average value when compared with the runoff function ($\mathcal{J}_n > B$).

In the limiting case of $A = 0$, the runoff at each hillslope would be a sinusoidal wave of amplitude C and average value B taking the form $R = B + C\sin(2\pi\nu t)$. Then, the solution at the outlet becomes

$$q_i = \sum_{n=1}^{D_i} W_n^{(i)} [\mathcal{J}_n + \mathcal{K}_n \sin(2\pi\nu(t-\theta_n))] + e^{-kt} \sum_{n=1}^{D_i} W_n^{(i)} \sum_{j=0}^{n-1} \mathcal{L}_{n-j} \frac{(kt)^j}{j!}, \tag{16}$$

where $\mathcal{K}_n$, $\mathcal{J}_n$, and θ are defined by $\mathcal{K}_j = C\prod_{i=1}^{j} \frac{k}{\sqrt{k^2+4\pi^2\nu^2}}$, $\mathcal{J}_j = B$, and $\sin(2\pi\nu\theta) = \frac{2\pi\nu}{\sqrt{k^2+2\pi^2\nu^2}}$ and $\cos(2\pi\nu\theta) = \frac{k}{\sqrt{k^2+2\pi^2\nu^2}}$.

HESSD
12, 8175–8220, 2015

It is apparent that the second sum of Eq. (16) that includes exponential decay at the rate of water movement through the river link is the transient term. The first sum of Eq. (16) is the asymptotic solution and includes the sum of constant terms from each hillslope and the sum of amplitudes of the sine waves from each hillslope. Following a similar approach in the case of $A > 0$ and using the fact that $A \ll k$, we again find that the second term in Eq. (15) decays much faster and, consequently, $e^{-At} \sum_{n=1}^{D_i} W_n^{(i)}[\mathcal{J}_n + \mathcal{K}_n \sin(2\pi \nu(t - \theta_n))]$ can be interpreted as being the asymptotic solution of q_i. Due to interference from sinusoidal waves that can be in or out of phase, the amplitude of the asymptotic solution in q_i can change depending on the phase shift. We investigate this dependence in Sect. 3.2.

2.2 Analytic solution extended to nonuniform k in the river network

In order to apply this work to river networks of different scales, we must consider the case in which each link is permitted to differ significantly from other links nearby or along the same path to the network outlet. The physical properties that represent these differences are the river link-length and stream velocity. River links of large magnitude tend to have higher velocities but can have a small link-length compared to river links with small magnitudes (and subsequent low velocities). Certainly, the magnitudes along any path are strictly increasing, so the velocity is expected to strictly increase as we trace a path from any river link to the river network outlet.

The transport equation given by Eq. (2) contains the constant rate, k_n, which is different for each link. Using the given baseflow pattern from Eq. (1)–which has been selected based on observed streamflow (Wondzell et al., 2007)–the transport equation can be written as

$$\frac{\mathrm{d}q_n}{\mathrm{d}t} = k_n\left[q_{\mathrm{in}_1} + q_{\mathrm{in}_2} + Be^{-At} + Ce^{-At}\sin(2\pi\nu t) - q_n\right]$$

HESSD
12, 8175–8220, 2015

or just

$$\frac{dq_n}{dt} = k_n[f_n(t) - q_n]. \quad (17)$$

Without loss of generality, we will seek to find the streamflow at the outlet of a given river network. In order to determine the streamflow at any distinct location in a river network (not limited to the outlet), one can simply consider the point of interest to be the outlet of a river network formed by all links upstream and follow the same procedure.

To compute the streamflow at the outlet of the river network, we will separately consider the influence of the runoff on each hillslope in the river network, as we have done in the uniform k case. We will trace this runoff downstream to the outlet for each hillslope in the network then take the sum over all links in the stream to determine the total flow at the river outlet.

Without uniform conditions, the complete solution for streamflow at the outlet cannot be written in a way that includes the width function. For that reason, we will offer only the partial solution derived from tracing runoff from one hillslope down a single path. For the development of this solution, we implement the following steps:

2.2.1 Solving the linear transport equation for the first link

The transport equation is a nonhomogeneous linear ordinary differential equation, but, in this case, the linear rate k is different for each link so that the transport equation for a given link is of the form Eq. (17). The solution at the outlet of the first link is nearly identical to that in the uniform k case (see Appendix A) but will be arranged slightly differently to accommodate different links along the path. Based on Eq. (17), the streamflow at the outlet of the first link is

$$q_1(t) = q_1(0)e^{-k_1 t} + \int_0^t k_1 f_1(s) e^{-k_1(t-s)} ds \quad (18)$$

HESSD
12, 8175–8220, 2015

where $f_1(t) = Be^{-At} + Ce^{-At}\sin(2\pi\nu t)$ is a representation of baseflow runoff at the hillslope scale. As in the uniform k case, Eq. (18) is solved using integration by parts, and the resulting flow at the outlet of the first link is:

$$q_1(t) = \left(q_1(0) + \frac{k_1}{\sqrt{(k_1 - A)^2 + 4\pi^2\nu^2}} C\sin(2\pi\nu\theta_1) \right) e^{-k_1 t} + k_1 B \frac{e^{-At} - e^{-k_1 t}}{k_1 - A}$$
$$+ \frac{k_1}{\sqrt{(k_1 - A)^2 + 4\pi^2\nu^2}} C\sin(2\pi\nu(t - \theta_1))e^{-At}.$$

Each term above is well defined due to physical restrictions on each parameter. Since ν represents the frequency of the daily cycle of evapotranspiration, this frequency is fixed to correspond to a period of 24 h. The values of k_1 and A represent the inverse of the residence time in river link 1 and in the hillslope adjacent to link 1, respectively. Since water moves significantly more slowly through the hillslope subsurface than along the stream, we expect the value of k_1 to be significantly larger than A. This means that the value of $\frac{k_1}{k_1 - A}$ is slightly greater than 1, while the value of $\frac{k_1}{\sqrt{(k_1 - A)^2 + 4\pi^2\nu^2}}$ is smaller than 1.

Let us now define the following quantities: $\mathcal{K}_n = C\prod_{j=1}^{n} \frac{k_j}{\sqrt{(k_j - A)^2 + 4\pi^2\nu^2}}$, $\mathcal{L}_n = q_n(0) + \mathcal{K}_n \sin(2\pi\nu\Phi_n)$, $\Phi_n = \sum_{j=1}^{n} \theta_j$ with θ_j $(j \geq 1)$ defined by

$$\sin(2\pi\nu\theta_j) = \frac{2\pi\nu}{\sqrt{(k_j - A)^2 + 4\pi^2\nu^2}}$$
$$\cos(2\pi\nu\theta_j) = \frac{k_j - A}{\sqrt{(k_n - A)^2 + 4\pi^2\nu^2}}. \quad (19)$$

HESSD
12, 8175–8220, 2015

In addition, if we consider the runoff to be the "zero step" along the path, then the "streamflow" there can be defined as $q_0(t) = Be^{-At} + Ce^{-At}\sin(2\pi\nu t)$. Then, for q_0, we define $\mathcal{K}_0$, Φ_0 and $\mathcal{L}_0$ by convention as: $\mathcal{K}_0 = B$, $\Phi_0 = \theta_0 = 0$, and $\mathcal{L}_0 = B$, as well as $q_0(0) = B$, $k_0 = A$. Then, the streamflows q_0 and q_1 can be rewritten as:

$$q_0(t) = \mathcal{K}_0 \sin(2\pi\nu(t-\Phi_0))\, e^{-At} + \mathcal{L}_0 e^{-k_0 t} \tag{20}$$

$$q_1(t) = \mathcal{K}_1 \sin(2\pi\nu(t-\Phi_1))\, e^{-At} + \mathcal{L}_1 e^{-k_1 t} - k_1\mathcal{L}_0 \frac{e^{-k_1 t} - e^{-k_0 t}}{k_1 - k_0}. \tag{21}$$

The time delay and coefficients $\mathcal{K}_n$ can be defined recursively by formulas

$$\Phi_{n+1} = \Phi_n + \theta_{n+1}$$

$$\mathcal{K}_{n+1} = \mathcal{K}_n \frac{k_{n+1}}{\sqrt{(k_{n+1} - A)^2 + 4\pi^2\nu^2}}.$$

2.2.2 Propagating oscillations through multiple river links

To propagate the volume of water downstream, the streamflow q_1 enters the *second link* as upstream input with no additional input from runoff in link 2. Because the k values are different for the two links, the resulting flow contains the distinct values k_1 and k_2, and the resulting streamflow solution after two links is

$$\begin{aligned} q_2(t) = {} & \mathcal{K}_2 \sin(2\pi\nu(t-\Phi_2))\, e^{-At} \\ & + \mathcal{L}_2 e^{-k_2 t} \\ & - k_2\mathcal{L}_1 \left(\frac{e^{-k_2 t} - e^{-k_1 t}}{k_2 - k_1} \right) \\ & + k_1 k_2 \mathcal{L}_0 \frac{\left(\frac{e^{-k_2 t} - e^{-k_1 t}}{k_2 - k_1}\right) - \left(\frac{e^{-k_2 t} - e^{-k_0 t}}{k_2 - k_0}\right)}{k_1 - k_0}. \end{aligned} \tag{22}$$

HESSD
12, 8175–8220, 2015

Notice the number of terms in the streamflow solution at each level. The preliminary flow, $q_0(t)$, given in Eq. (20), contains two terms: one with an exponential function and one with a sinusoidal wave multiplied by an exponential function. The flow after one link, $q_1(t)$ from Eq. (21), contains a total of four terms: the exponentially decaying sinusoid and the other 3 exponential terms. (We count each exponential function separately, $e^{-k_2 t}$, $e^{-k_1 t}$, and $e^{-k_0 t}$.) Then, the streamflow after two links, q_2, contains eight terms total. Therefore, we expect this trend to continue so that the streamflow after n links would contain 2^{n+1} terms.

To confirm this, let us calculate

$$q_3(t) = q_3(0)e^{-k_3 t} + k_3 e^{-k_3 t}\int_0^t q_2(s)e^{k_3 s}\mathrm{d}s,$$

and obtain

$$\begin{aligned}
q_3(t) &= \mathcal{K}_3 \sin(2\pi\nu(t-\Phi_3))\,e^{-At} + \mathcal{L}_3 e^{-k_3 t} \\
&- k_3\mathcal{L}_2 \frac{e^{-k_3 t} - e^{-k_2 t}}{k_3 - k_2} \\
&+ \frac{\mathcal{L}_1 k_2 k_3}{k_2 - k_1}\left(\frac{e^{-k_3 t} - e^{-k_2 t}}{k_3 - k_2} - \frac{e^{-k_3 t} - e^{-k_1 t}}{k_3 - k_1}\right) \\
&- \frac{\mathcal{L}_0 k_1 k_2 k_3}{k_1 - k_0}\frac{1}{k_2 - k_1}\left(\frac{e^{k_3 t} - e^{-k_2 t}}{k_3 - k_2} - \frac{e^{-k_3 t} - e^{-k_1 t}}{k_3 - k_1}\right) \\
&+ \frac{\mathcal{L}_0 k_1 k_2 k_3}{k_1 - k_0}\frac{1}{k_2 - k_0}\left(\frac{e^{-k_3 t} - e^{-k_2 t}}{k_3 - k_2} - \frac{e^{-k_3 t} - e^{-k_0 t}}{k_3 - k_0}\right)
\end{aligned}$$

which, indeed has sixteen terms and therefore confirms the pattern.

HESSD
12, 8175–8220, 2015
On the propagation of diel signals in river networks using analytic solutions
M. Fonley et al.

By collecting like terms, an algorithmic description of the solution emerges:

$$q_0(t) = \mathcal{K}_0 \sin(2\pi\nu(t-\Phi_0))\, e^{-At} + \mathcal{L}_0 e^{-k_0 t}$$

$$q_1(t) = \mathcal{K}_1 \sin(2\pi\nu(t-\Phi_1))\, e^{-At} + \mathcal{L}_1 e^{-k_1 t} - k_1 \mathcal{L}_0 \left(\frac{e^{-k_1 t} - e^{-k_0 t}}{k_1 - k_0}\right)$$

$$q_2(t) = \mathcal{K}_2 \sin(2\pi\nu(t-\Phi_2))\, e^{-At} + \mathcal{L}_2 e^{-k_2 t} - k_2 \mathcal{L}_1 \left(\frac{e^{-k_2 t} - e^{-k_1 t}}{k_2 - k_1}\right)$$
$$+ k_2 k_1 \mathcal{L}_0 \left(\frac{\left(\frac{e^{-k_2 t} - e^{-k_1 t}}{k_2 - k_1}\right) - \left(\frac{e^{-k_2 t} - e^{-k_0 t}}{k_2 - k_0}\right)}{k_1 - k_0}\right)$$

$$q_3(t) = \mathcal{K}_3 \sin(2\pi\nu(t-\Phi_3))\, e^{-At} + \mathcal{L}_3 e^{-k_3 t} - k_3 \mathcal{L}_2 \left(\frac{e^{-k_3 t} - e^{-k_2 t}}{k_3 - k_2}\right)$$
$$+ k_3 k_2 \mathcal{L}_1 \left(\frac{\left(\frac{e^{-k_3 t} - e^{-k_2 t}}{k_3 - k_2}\right) - \left(\frac{e^{-k_3 t} - e^{-k_1 t}}{k_3 - k_1}\right)}{k_2 - k_1}\right)$$
$$- k_3 k_2 k_1 \mathcal{L}_0 \left(\frac{\left(\frac{\left(\frac{e^{-k_3 t} - e^{-k_2 t}}{k_3 - k_2}\right) - \left(\frac{e^{-k_3 t} - e^{-k_1 t}}{k_3 - k_1}\right)}{k_2 - k_1}\right) - \left(\frac{\left(\frac{e^{-k_3 t} - e^{-k_2 t}}{k_3 - k_2}\right) - \left(\frac{e^{-k_3 t} - e^{-k_0 t}}{k_3 - k_0}\right)}{k_2 - k_0}\right)}{k_1 - k_0}\right).$$

Based on the above observations, we are able to generalize and determine the nth term in the solution-sequence, $q_n(t)$, which is defined by the contribution from a hillslope of topological distance n upstream. This is the streamflow

HESSD
12, 8175–8220, 2015

$$q_n(t) = \mathcal{K}_n \sin(2\pi\nu(t-\Phi_n))\, e^{-At} + \sum_{j=0}^{n} P_{jn}\mathcal{L}_j\mathcal{F}_{(n-j),n}(t), \quad n \geq 1 \tag{23}$$

with coefficients $\mathcal{K}_n$, Φ_n, $\mathcal{L}_j$, and P_{jn} defined accordingly by Eq. (19) and

$$\mathcal{K}_n = C\prod_{j=1}^{n} \frac{k_j}{\sqrt{(k_j-A)^2 + 4\pi^2\nu^2}} \text{ for } j = 1,\, 2,\, \ldots,\, n$$

$$\Phi_n = \sum_{j=0}^{n} \theta_j$$

$$\mathcal{L}_j = q_j(0) + \mathcal{K}_j \sin\left(2\pi\nu\Phi_j\right)$$

$$P_{jn} = \prod_{i=j+1}^{n} (-k_i) \text{ for } j = 0,\, 1,\, \ldots,\, n-1$$

as well as $P_{nn} = 1$ and initial values $k_0 = A$, $\mathcal{K}_0 = C$, $\mathcal{L}_0 = B$, and $\theta_0 = 0$.

2.2.3 Assembling the streamflow solution using an algorithmic description

In order to fully describe solution (Eq. 23), we need to determine the values of $\mathcal{F}_{jn}(t)$, which can be computed algorithmically based on the following "tree"-like structure:

For given $n \geq 1$, we follow along the $(n+1)$-level tree starting with parents $f_0(t)$, $f_1(t)$, ..., $f_n(t)$ where $f_l(t) = e^{-k_l t}$ (see Fig. 4 for $n = 4$). Then, the values of $\mathcal{F}_{jn}$ are recursively calculated at each stage by:

$$\mathcal{F}_{jn}(t) := f_{n-j,n-j+1,\, \ldots,\, n}(t)$$

HESSD
12, 8175–8220, 2015

where

$$
\begin{array}{lll}
\text{For } j=0: & \text{take } l=\overline{0,n} \text{ and}: & f_l(t)=e^{-k_l t} \\
\text{For } j=1: & \text{take } l=\overline{0,n-1} \text{ and}: & f_{l,n}(t)=\frac{e^{-k_l t}-e^{-k_n t}}{k_l-k_n} \\
\text{For } j=2: & \text{take } l=\overline{0,n-2} \text{ and}: & f_{l,n-1,n}(t)=\frac{f_{l,n}(t)-f_{n-1,n}(t)}{k_l-k_{n-1}} \\
\text{For } j=3: & \text{take } l=\overline{0,n-3} \text{ and}: & f_{l,n-2,n-1,n}(t)=\frac{f_{l,n-1,n}(t)-f_{n-2,n-1,n}(t)}{k_l-k_{n-2}} \\
\text{For } j=4: & \text{take } l=\overline{0,n-4} \text{ and}: & f_{l,n-3,n-2,n-1,n}(t)=\frac{f_{l,n-2,n-1,n}(t)-f_{n-3,n-2,n-1,n}(t)}{k_l-k_{n-3}} \\
\vdots & & \\
\text{For } j=n: & l=0 & f_{0,1,2,\ldots,n}(t)=\frac{f_{0,2,\ldots,n}-f_{1,2,\ldots,n}}{k_0-k_1}.
\end{array}
$$

Therefore, we can rewrite q_0, q_1, q_2, and q_3 as

$$
\begin{aligned}
q_0 &= \mathcal{K}_0 \sin(2\pi\nu(t-\Phi_0))\, e^{-At} + \mathcal{L}_0 f_0 \\
q_1 &= \mathcal{K}_1 \sin(2\pi\nu(t-\Phi_1))\, e^{-At} + \mathcal{L}_1 f_1 - \mathcal{L}_0 k_1 f_{01} \\
q_2 &= \mathcal{K}_2 \sin(2\pi\nu(t-\Phi_2))\, e^{-At} + \mathcal{L}_2 f_2 - \mathcal{L}_1 k_2 f_{12} + \mathcal{L}_0 k_1 k_2 f_{012} \\
q_3 &= \mathcal{K}_3 \sin(2\pi\nu(t-\Phi_3))\, e^{-At} + \mathcal{L}_3 f_3 - \mathcal{L}_2 k_3 f_{23} + \mathcal{L}_1 k_2 k_3 f_{123} - \mathcal{L}_0 k_1 k_2 k_3 f_{0123}.
\end{aligned}
$$

Applying the algorithmic tree to our streamflow at link 4 (for example) at this point, we recognize that

$$
\begin{aligned}
q_4(t) = {} & \mathcal{K}_4 \sin(2\pi\nu(t-\Phi_4))\, e^{-At} + \mathcal{L}_4 f_4 - \mathcal{L}_3 k_4 f_{34} + \mathcal{L}_2 k_3 k_4 f_{234} - \mathcal{L}_1 k_2 k_3 k_4 f_{1234} \\
& + \mathcal{L}_0 k_1 k_2 k_3 k_4 f_{01234}.
\end{aligned}
$$

While the algorithm may seem complicated to follow, it has a very easy coding implementation. In Appendix B, we include the Matlab code lines that describe the algorithm.

HESSD

12, 8175–8220, 2015

On the propagation of diel signals in river networks using analytic solutions

M. Fonley et al.

3 Results

3.1 Experimental setup: testing the effects of velocity on streamflow amplitude and time delay downstream

In order to test the competing hypotheses by Wondzell et al. (2007) and those presented in Graham et al. (2013), we will demonstrate the amplification and damping of the oscillatory streamflow signal that are caused by superposition. We consider a sample network and compute the streamflow solution at different locations in the river network when the velocity and its corresponding time delay are varied. We will consider both the uniform (with $v_i = v$ for all links i) and the variable velocity cases.

We compute the streamflow solution for the Mandelbrot-Viscek tree of magnitude 14, as shown in Fig. 5. The Mandelbrot-Vicsek tree is self-similar (Mandelbrot and Vicsek, 1989) and has been used to demonstrate hydrologic properties at different scales (Mantilla et al., 2006; Peckham, 1995), for example. In this figure, the label next to each link represents the magnitude of the link, which is determined by the sum of the magnitudes of the two immediate upstream 'parent' links where external links have magnitude 1. The constant parameter values used in this example are $A = 1.2 \times 10^{-4}$ [h^{-1}], $B = 0.08$ [$\mathrm{L\,s}^{-1}$], $C = 0.008$ [$\mathrm{L\,s}^{-1}$], $q_0 = 0.08$ [$\mathrm{L\,s}^{-1}$], and $v = \frac{1}{24}$ [h^{-1}] and are uniform over each link in the network. To test the effects of superposition on streamflow, we will simulate streamflow for different transport constants k. Figure 6 shows the simulation runoff pattern (top) along with the sample streamflow solution at the outlet of the network in the uniform case (bottom). To distinguish among the different simulations, we will narrow our view to a few oscillations, which are highlighted by a box in the panels in Fig. 6.

3.2 Uniform velocity over the river network

In the case of uniform velocities, the streamflow at the outlet is given by the solution to Eq. (15). The time delay depends upon parameters that have physically-based val-

HESSD
12, 8175–8220, 2015

On the propagation of diel signals in river networks using analytic solutions

M. Fonley et al.

ues (see Eq. 6), so a realistic range for the time delay and phase shift can be found. These parameters, k and A, are incorporated in other parts of the solution (see Eq. 8). Therefore, changing their values impacts the solution in more ways than just the superposition of sinusoidal functions. The physical value represented by A is expected to remain constant for a given region. On the other hand, k represents the inverse of the residence time in each river link and is not necessarily uniform or fixed.

Recall that k is given by $\frac{v}{l}$, where v is the stream velocity and l is the stream length. The length of each river link in a real river network would be different, as would the velocity. In addition, the velocity may change over time, since velocity increases with flow. Consequently, the realistic value of k is expected to be different for each link in the network, and the uncertainty of k is a possible source for different time delays and phase shifts.

While the effect of varying k is not limited to the time delay, the value of k also affects $\mathcal{K}_n$ and $\mathcal{J}_n$ (see Eq. 8). Note that the coefficient $\mathcal{J}_n$ determines the average value of the streamflow solutions, while the coefficient $\mathcal{K}_n$ determines the amplitude of the oscillation in each step of the streamflow solution (see Eq. 15 – first term). Changing k, then, impacts the amplitude downstream more significantly than simply altering the time delay and subsequent phase shift.

The results of simulating streamflow in the Madelbrot–Viscek tree using different values of k can be found in Fig. 7. The values of k used in simulations are [0.38, 0.7, 1.02, 1.34, 1.66, 1.98, and 2.30] with resultant time delays of [2.30, 1.36, 0.95, 0.73, 0.59, 0.5, and 0.43] hours. The corresponding graph-solutions from Fig. 7 are drawn in the following colors: black, blue, green, cyan, orange, red, and purple, respectively. Each panel in Fig. 7 represents the solution at a different location along the network (refer to Fig. 5 for sample locations). We chose the timing of the plots so that a cyclic pseudo-equilibrium has been reached and the effects of time delay can be distinguished. For comparison among the different locations, we have normalized the flows about the average flow. The average flows at a link of each magnitude are plotted in Fig. 8 and, as

Discussion Paper | Discussion Paper | Discussion Paper | Discussion Paper |

HESSD

12, 8175–8220, 2015

On the propagation of diel signals in river networks using analytic solutions

M. Fonley et al.

expected, the values depend upon the number of links upstream, which is related to the magnitude of the link.

From Fig. 7, we see that the magnitude of the oscillations can be significantly decreased as velocity and k decrease, because this represents a volume of water spending more time in any one link. This causes a greater time delay, which means that two links will combine their flows out of phase, and superposition dictates that the amplitude of the resulting oscillations is decreased. Furthermore, a lower velocity leads to significant attenuation of the streamflow along each link in the network. The greatest amplitudes occur when the velocity is highest, which moves a volume of water very quickly through each link and leads to very little loss of streamflow intensity. Notice also that the timing of the peak streamflow is increasingly delayed as velocity slows (see Fig. 7 for $k = 0.38$, 1.02, and 1.66, for example). This can explain the increasing time delay that has been observed between maximum evapotranspiration and minimum streamflow as the dry season progresses. These results also indicate that the time delay increases continuously as the velocity decreases continuously over time so that the time delay can be predictable depending upon stream velocity.

At the link of magnitude 1, the phase shift has little influence on the amplitude and only has an influence on the timing of the wave. At the outlet of a magnitude-2 link, the two upstream links are "in phase", meaning they have the same time delay as each other since they are the same topological distance from the point at which we compute streamflow. Therefore, these two will exhibit constructive interference. When they are combined with the downstream link, however, the different values of phase shift can result in constructive or destructive interference, although they never completely destroy the oscillations. The phase shift that produces the maximum streamflow is zero because this represents the fact that all three streamflows that feed into this outlet are completely in phase.

As we examine the streamflows in links with greater magnitude, the shape of the network (described by the width function) becomes important because the flows from all links of a given distance will reach the outlet at the same time. Being out of phase with

HESSD
12, 8175–8220, 2015

links of other distances can cause some reduction in the amplitude of the streamflow oscillations, but the oscillations will not be completely destroyed.

3.3 Variable velocity over the river network

To illustrate our results, we will now apply the algorithm from Sect. 2.2.3 at the outlet of the Mandelbrot-Viscek tree from Fig. 5 using the same values for A, B, C, and v as in Sect. 3.2. However, we will assume that each link length is fixed but that the velocity grows logarithmically with the magnitude of the river link. Another complication is that in order to find the total streamflow at the outlet, we can no longer utilize the width function because the strategy from Sect. 2 relied upon the assumption that the partial streamflow from links of the same distance from the outlet are the same. In the nonuniform case not only the length of the path, but also the specific path are important. Our strategy now is to trace the runoff from all upstream hillslopes.

$$q_{\text{outlet}}(t) = \sum_{\text{upstream links}} \left[\mathcal{K}_n \sin(2\pi v(t-\Phi_n))\, e^{-At} + \sum_{j=0}^{n} P_{jn}\mathcal{L}_j\mathcal{F}_{(n-j),n}(t) \right] \tag{24}$$

In Eq. (24), the value of n changes for every link, which represents the length of the path from that link to the outlet.

Using Eq. (24), we compute the solution at the outlet of the Mandelbrot-Viscek tree of magnitude 14 (Fig. 5) for different maximum velocities in the network. In each simulation, the velocity of a given link depends logarithmically upon the link's magnitude, as seen in Fig. 9. The resulting normalized flows at the outlet are shown in Fig. 10, where the maximum velocities used in simulations are [0.016, 0.066, 0.12, 0.17, 0.22, 0.27, and 0.32] [$\text{m}\,\text{s}^{-1}$]. The corresponding k values are [0.11, 0.47, 0.84, 1.20, 1.56, 1.92, and 2.28] [h^{-1}]. The corresponding graph-solutions from Fig. 10 are drawn in the following colors: black, blue, green, cyan, orange, red, and purple, respectively. Although k is no longer uniform over the river network, we again see the pattern in which decreasing k lowers the magnitude of oscillations at the outlet and causes a greater

HESSD
12, 8175–8220, 2015

time delay in the peak values. Physically, these results mean that a decrease in each distinct k value over the whole river network (as would happen under dry conditions when the velocity decreases over time) leads to a greater time delay and smaller peak values in the oscillation due to the superposition of streamflow oscillations from each link. This supports the hypotheses of Wondzell et al. (2007) to describe streamflow patterns observed under dry conditions.

3.4 Propagation of the analytic solution on a real network

In this section, we apply the analytic streamflow solution for uniform conditions to a more complex river network to see the effects of scale on streamflow amplitude and timing. In the previous section, we also examined the flow at different scales (see Fig. 7) but with an emphasis on different k values. The time range in Fig. 7 has been decreased, and the flows have been normalized about their average value to exaggerate the effects of changing the k value. Consider the blue line in all panels of Fig. 7 corresponding to a k value of $0.7\,h^{-1}$. Streamflow at a larger scale (magnitude) is influenced by a greater number of upstream links. Then, superposition effects among those upstream links are stronger and we see two resulting attributes in the streamflow properties: reduction in the streamflow amplitude and greater time delay to the peak. We now consider a larger, more realistic river network and expect to see similar results.

The network we use for streamflow simulations is the Dry Creek watershed in Idaho, which has an area of $169.25\,km^2$ and can be seen in Fig. 11. To facilitate the large number of computations, we use the asynchronous solver introduced in Small (2013) and used in Mantilla and Cunha (2012). The watershed contains river links at scales of up to Horton order 7. For details regarding Horton order, see Rodriguez-Iturbe and Rinaldo (2001). We simultaneously apply the runoff pattern described in Sect. 3 to each hillslope in the network and examine the resulting streamflow at links of different orders.

In our theoretical examples, we assumed the length of each link to be uniform over the river network, so that changes in velocity directly correspond to changes in the

HESSD
12, 8175–8220, 2015

transport constant k. Realistic network parameters include variable link-length, so we vary the velocity of each link accordingly in order to maintain a uniform k value and apply the solution developed in Sect. 2.1. The runoff pattern and resulting streamflows at links of different order along the river network can be found in Fig. 12. Note that these flows are not normalized. For links of larger orders, superposition among the upstream links causes the amplitude of the streamflow oscillations to be so small that they are nearly indistinguishable.

To emphasize the time delay at different orders, we have included a line highlighting the time to a corresponding peak in each panel of Fig. 12. As shown in Fig. 12, while, in practice we cannot say the highlighted peak is the *same* peak propagated downstream, in theory, these corresponding peaks are consistent with the analytic solution given in Sect. 2.1, which describes a strictly increasing time delay.

4 Conclusions and future work

Observations of oscillatory streamflow during low flow conditions have highlighted the magnitude and time delay caused by the diel signal that represents evapotranspiration. Several current hypotheses suggest that the properties of the oscillatory streamflow signal can be attributed to different methods of water movement through the subsurface, although another hypothesis suggests that flow along the river determines the timing and amplitude of oscillations. In this paper, we provide evidence to support the latter argument.

First, we select a mathematical function according to streamflow observations at the catchment scale to represent baseflow patterns at the hillslope scale. The selected baseflow pattern is applied as input to a linear transport equation for all links in a river network that are assumed to have uniform properties and parameter values. For this uniform situation, we develop an analytic solution to represent streamflow at any point in a river network. We compute the solution by separately determining the partial streamflow at the outlet from each river link then taking the sum over all river links in the river network. In order to include the geomorphology of the river network, we use the width function to compute the complete streamflow solution. We have also extended the streamflow solution to include nonuniform links in the river network.

The solution for streamflow contains a collection of sine functions, each of which exhibits a phase shift determined by the topological distance of the corresponding hillslope from the outlet. We have shown that the physical parameters that determine the phase shift have a great impact on the streamflow as it propagates downstream. The streamflows computed using different physical parameters demonstrate that the decreasing amplitude and increasing time delay in observed streamflows can be attributed to the decreasing velocity in the river network during dry conditions, and they are not necessarily due to soil-water processes, as was previously thought, which supports the hypothesis of Wondzell et al. (2007). Furthermore, the structure of the analytic solution indicates that the time delay increases continuously as the river network velocity continuously decreases, so that the time delay can be predictable depending on stream velocity. The results are consistent in both the uniform and nonuniform parameter cases. We also observe consistent results with the streamflow amplitude and timing at links of different orders in a more complex and realistic network. Our results, however, do not disprove the hypothesis that delays can come from subsurface flow processes.

As a next step, we propose to test the analytic solutions herein on networks with different geomorphological structures in order to compare the resulting streamflow amplitudes and emphasize the dependence upon network geometry. We suggest subsequently comparing our analytic solutions with the numerical results obtained using nonlinear transport equations, which will demonstrate the relationship between link propagation at the hillslope scale and streamflow at the catchment scale. Careful field experiments would be necessary to provide a definitive conclusion about the attribution of time delays.

HESSD
12, 8175–8220, 2015

Appendix A: Development of streamflow solution for uniform k value over all links in the river network

In order to simplify our calculations below, we will use the notation $\omega = 2\pi\nu$.

We prove Eq. (7) from Sect. 2.1.1 by using the method of mathematical induction. The isolated effects of runoff from link i on links downstream are found by applying the transport equation

$$\frac{\mathrm{d}q_i(t)}{\mathrm{d}t} = k(Be^{-At} + Ce^{-At}\sin(\omega t) - q_i(t)). \tag{A1}$$

We did not include in Eq. (A1) any upstream links because we are trying to isolate the effects on streamflow due to runoff from hillslope i. Therefore, we treat it as an external link. Equation (A1) is a nonhomogeneous linear ordinary differential equation of the form

$$\frac{\mathrm{d}q_i}{\mathrm{d}t} = kf_i(t) - kq_i, \tag{A2}$$

and has the solution

$$q_i(t) = q_i(0)e^{-kt} + ke^{-kt}\int_0^t f_i(s)e^{ks}\mathrm{d}s. \tag{A3}$$

As we trace the runoff downstream, the function $f_i(t)$ is the input to the link, which can come from upstream sources or from runoff from the adjacent hillslope. Since link i is arbitrary, we will consider it to be the first link in a path to the outlet, so it will be labeled link 1 having flow q_1, and the next link downstream will be labeled link 2, etc. Since $f_1(t)$ consists only of baseflow, the solution q_1 according to Eq. (A3) becomes

$$q_1(t) = q_1(0)e^{-kt} + ke^{-kt}\int_0^t \left[Be^{(k-A)s} + Ce^{(k-A)s}\sin(\omega s)\right] \mathrm{d}s$$

$$= q_1(0)e^{-kt} + Bke^{-kt}\left(\frac{e^{(k-A)t}}{k-A} - \frac{1}{k-A}\right) + Cke^{-kt}\int_0^t e^{(k-A)s}\sin(\omega s)\mathrm{d}s. \quad \text{(A4)}$$

The solution to the latter integral is

$$\int_0^t e^{(k-A)s}\sin(\omega s)\mathrm{d}s = \frac{e^{(k-A)t}}{\sqrt{(k-A)^2+\omega^2}}\sin(\omega t - \varphi) + \frac{\sin(\varphi)}{\sqrt{(k-A)^2+\omega^2}},$$

and φ is defined by its sine and cosine functions

$$\sin(\varphi) = \frac{\omega}{\sqrt{(k-A)^2+\omega^2}}$$
$$\cos(\varphi) = \frac{k-A}{\sqrt{(k-A)^2+\omega^2}}.$$

Substituting this integral back into Eq. (A4), we obtain

$$q_1(t) = \left(q_1(0) - \frac{k}{k-A}B + \frac{k}{\sqrt{(k-A)^2+\omega^2}}C\sin\varphi\right)e^{-kt}$$
$$+ \left(\frac{k}{k-A}B + \frac{k}{\sqrt{(k-A)^2+\omega^2}}C\sin(\omega t - \varphi)\right)e^{-At}. \quad \text{(A5)}$$

HESSD
12, 8175–8220, 2015
On the propagation of diel signals in river networks using analytic solutions
M. Fonley et al.

To find an algorithmic method to compute the coefficients of the solution $q_n(t)$ for $n \geq 1$, we define the following:

$$\mathcal{K}_n := C\prod_{j=1}^{n}\frac{k}{\sqrt{(k-A)^2+\omega^2}} \qquad n \geq 1 \tag{A6}$$

$$\mathcal{J}_n := B\prod_{j=1}^{n}\frac{k}{k-A} \qquad n \geq 1 \tag{A7}$$

$$\Phi_n := \sum_{j=1}^{n}\varphi \qquad n \geq 1 \tag{A8}$$

$$\mathcal{L}_j := q_j(0) - \mathcal{J}_j + \mathcal{K}_j \sin\left(\Phi_j\right) \qquad j = 1, \ldots, n. \tag{A9}$$

Using these newly defined quantities from Eqs. (A6)–(A9), the flow at the outlet of link 1 can be rewritten as

$$q_1 = \mathcal{L}_1 e^{-kt} + e^{-At}\left[\mathcal{J}_1 + \mathcal{K}_1 \sin(\omega t - \Phi_1)\right]. \tag{A10}$$

To find the solution for the next link downstream (link 2), the flow from link 1, given by Eq. (A10), is included as q_{in_1} as the transport Eq. (2) is applied to link 2. Integration by parts will again be used to find the solution to

$$\frac{\mathrm{d}q_2}{\mathrm{d}t} = k\left(q_1 - q_2\right).$$

Discussion Paper | Discussion Paper | Discussion Paper | Discussion Paper |

HESSD

12, 8175–8220, 2015

On the propagation of diel signals in river networks using analytic solutions

M. Fonley et al.

Using Eq. (A3),

$$q_2(t) = q_2(0)e^{-kt} + ke^{-kt}\int_0^t q_1(s)e^{ks}\mathrm{d}s$$

$$= q_2(0)e^{-kt} + ke^{-kt}\mathcal{L}_1 t + ke^{-kt}\mathcal{J}_1\left(\frac{e^{(k-A)t}}{k-A} - \frac{1}{k-A}\right)$$

$$+ ke^{-kt}\mathcal{K}_1\int_0^t e^{(k-A)s}\sin(\omega s - \Phi_1)\mathrm{d}s. \quad \text{(A11)}$$

The integral in Eq. (A11) is very similar to that in Eq. (A4), with the only differences being the argument of the sine function in the initial integral. After integration by parts, the equation for streamflow $q_2(t)$ becomes

$$q_2 = q_2(0)e^{-kt} + ke^{-kt}\mathcal{L}_1 t + ke^{-kt}\mathcal{J}_1\left(\frac{e^{(k-A)t}}{k-A} - \frac{1}{k-A}\right)$$

$$+ ke^{-kt}\mathcal{K}_1\left(\frac{1}{\sqrt{(k-A)^2+\omega^2}}\left(e^{(k-A)t}\sin(\omega t - \Phi_2) + \sin(\Phi_2)\right)\right)$$

or, equivalently,

$$q_2 = [\mathcal{L}_2 + kt\mathcal{L}_1]e^{-kt} + [\mathcal{J}_2 + \mathcal{K}_2\sin(\omega t - \Phi_2)]e^{-At}. \quad \text{(A12)}$$

By mathematical induction, using the same strategy for calculations along the path to the river network outlet, we can compute the contribution of runoff from any river link on flow at the outlet. For a given link that is at topological distance n from the outlet (or an alternative location from which flow is observed), its contribution to the flow at the outlet is:

HESSD
12, 8175–8220, 2015

$$q_n(t) = e^{-At}\left[\mathcal{J}_n + \mathcal{K}_n \sin(\omega t - \Phi_n)\right] + e^{-kt}\sum_{j=0}^{n-1} \mathcal{L}_{n-j}\frac{(kt)^j}{j!}. \tag{A13}$$

Given that $\omega = 2\pi\nu$ and using the notation $\varphi = 2\pi\nu\theta$, Eqs. (6)–(9) immediately will result.

Appendix B: Matlab code to compute $\mathcal{F}_{jn}(t)$

```
% In the following code, we use the convention: t is a column vector of p-time values
% t=[t1, t2, ..., tp]^T
% and kV is a row vector of (n+1) values [k0, k1, k2, ..., kn]
%%
% Create a matrix with p rows and (n+1) columns by repeating a copy of kV
%  k=[ k0 k1 k2... kn
%       k0 k1 k2... kn
%       ...
%       k0 k1 k2... kn]
%
% and another matrix with p rows and (n+1) columns of time values by repeating a
% copy of t
% time=[t1 t1 ... t1
%         t2 t2 ... t2
%         ...
%         tp tp ... tp]
% The resulting coefficient is the matrix with p rows and (n+1) columns given by:
%      [F_nn(t1) F_(n-1)n(t1) ... F_0n(t1)
%       F_nn(t2) F_(n-1)n(t2) ... F_0n(t2)
%       ...
```


HESSD
12, 8175–8220, 2015
On the propagation of diel signals in river networks using analytic solutions
M. Fonley et al.

```
%       F_nn(tp) F_(n-1)n(tp) ... F_0n(tp)]

function coeffMatrix=computeF(t,kV)
coeffMatrix=[];
k=repmat(kV,length(t),1);
time=repmat(t,1,length(kV));

f=exp(-time.*k);
fLast=f(:,end);
kLast=k(:,end);
coeffMatrix=[fLast coeffMatrix];
while size(f,2)>=2
f=f(:,1:end-1);
k=k(:,1:end-1);
f=(f-repmat(fLast,1,size(f,2)))./(k-repmat(kLast,1,size(f,2)));
fLast=f(:,end);
kLast=k(:,end);
coeffMatrix=[fLast coeffMatrix];
end
```

References

Arnell, N.: The effect of climate change on hydrological regimes in Europe: a continental perspective, Global Environ. Change, 9, 5–23, 1998. 8177

Bond, B., Jones, J., Moore, G., Phillips, N., Post, D., and McDonnell, J.: The zone of vegetation influence on baseflow revealed by diel patterns of streamflow and vegetation water use in a headwater basin, Hydrol. Process., 16, 1671–1677, 2002. 8176

Burn, D., Buttle, J., Caissie, D., MacCulloch, G., Spence, C., and Stahl, K.: The Processes, Patterns and Impacts of Low Flows Across Canada, Can. Water Resour. J., 33, 107–124, 2008. 8177
Burt, T. P.: Diurnal variations in stream discharge and throughflow during a period of low flow, J. Hydrol., 41, 291–301, 1979.
Graham, C., Barnard, H., Kavanagh, K., and McNamara, J.: Catchment scale controls the temporal connection of transpiration and diel fluctuations in streamflow, Hydrol. Process., 27, 2541–2556, 2013. 8176, 8177, 8194
Gribovszki, Z., Kalicz, P., Szilagyi, J., and Kucsara, M.: Riparian zone evapotranspiration estimation from diurnal groundwater level fluctuations, J. Hydrol., 349, 6–17, 2008. 8176
Gribovszki, Z., Szilagyi, J., and Kalicz, P.: Diurnal fluctuations in shallow groundwater levels and streamflow rates and their interpretation – A review, J. Hydrol., 385, 371–383, 2010. 8176
Mandelbrot, B. B. and Vicsek, T.: Directed recursive models for fractal growth, J. Phys. A, 22, L377–L383, 1989. 8194
Mantilla, R., Gupta, V., and Mesa, O.: Role of coupled flow dynamics and real network structures on Hortonian scaling of peak flows, J. Hydrol., 322, 155–167, 2006. 8194
Mantilla, R., Gupta, V. K., and Troutman, B. M.: Scaling of peak flows with constant flow velocity in random self-similar networks, Nonlin. Processes Geophys., 18, 489–502, doi:10.5194/npg-18-489-2011, 2011. 8179, 8184
Mantilla, R., Cunha, L. K., Krajewski, W. F., Small, S. J., Jay, L. O., Fonley, M., and Curtu, R.: Simulation of a distributed flood control system using a parallel asynchronous solver for systems of ODEs, Proceeding Applied Simulation and Modelling/777 Artificial Intelligence and Soft Computing, ACTA Press, Calgary, AB, Canada, doi:10.2316/P.2012.776-042, 2012. 8198
Mul, M., Kemerink, J., Vyagusa, N., Mshana, M., van der Zaag, P., and Makurira, H.: Water allocation practices among smallholder farmers in the South Pare Mountains, Tanzania: The issue of scale, Agr. Water Manage., 98, 1752–1760, 2011. 8177
Peckham, S.: New results for self-similar trees with applications to river networks, Water Resour. Res., 31, 1023–1029, 1995. 8194
Rodriguez-Iturbe, I. and Rinaldo, A.: Fractal river basins: chance and self-organization, Cambridge University Press, 2001. 8198

HESSD
12, 8175–8220, 2015

On the propagation of diel signals in river networks using analytic solutions

M. Fonley et al.

Title Page
Abstract | Introduction
Conclusions | References
Tables | Figures
◀I | ▶I
◀ | ▶
Back | Close
Full Screen / Esc
Printer-friendly Version
Interactive Discussion

Small, S. J., Jay, L. O., Mantilla, R., Curtu, R., Cunha, L. K., Fonley, M., and Krajewski, W. F.: An asynchronous solver for systems of ODEs linked by a directed tree structure, Adv. Water Resour., 53, 23–32, 2013. 8198

Stott, R. E. and Burt, T. P.: Potassium chemistry of a small upland stream following a major drought, Hydrol. Process., 11, 189–201, 1997. 8177

Wondzell, S., Gooseff, M., and McGlynn, B.: Flow velocity and the hydrologic behavior of streams during baseflow, Geophys. Res. Lett., 34, L24404, doi:10.1029/2007GL031256, 2007. 8176, 8177, 8186, 8194, 8198, 8200

Wondzell, S., Gooseff, M., and McGlynn, B.: An analysis of alternative conceptual models relating hyperheic exchange flow to diel fluctuations in discharge during baseflow recesseion, Hydrol. Process., 24, 686–694, 2010.

HESSD

12, 8175–8220, 2015

On the propagation of diel signals in river networks using analytic solutions

M. Fonley et al.

HESSD
12, 8175–8220, 2015

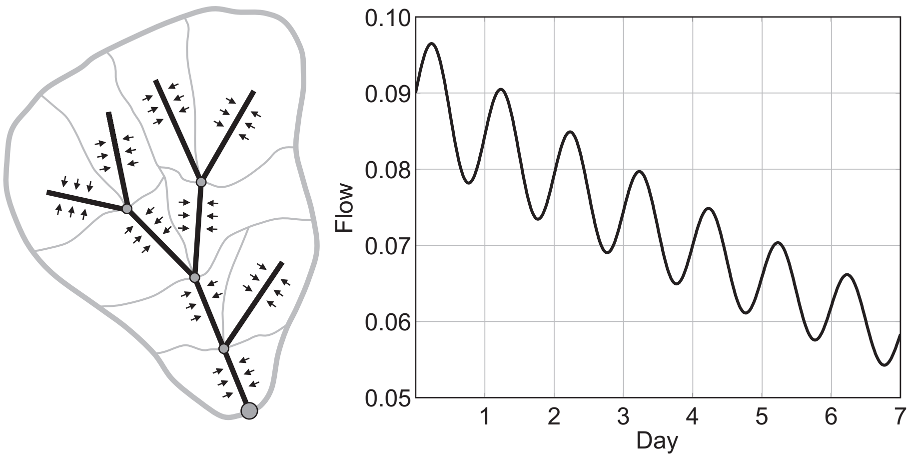

Figure 1. The left panel shows how runoff enters the river network as lateral flow from each hillslope to its adjacent link. The right panel shows a sample baseflow pattern given by Eq. (1) using $A = 0.003$ [h^{-1}], $B = 0.08$ [$L\,s^{-1}$], $C = 0.008$ [$L\,s^{-1}$], and $\nu = \frac{1}{24}$ [h^{-1}].

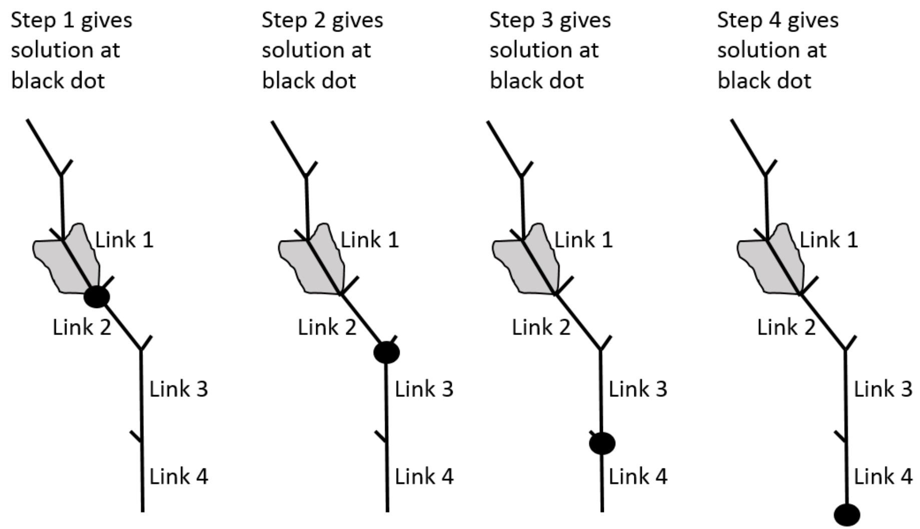

Figure 2. To determine the solution at any point, we consider runoff on only one hillslope (adjacent to link 1 in this case), and we trace the effects of that runoff downstream with no additional runoff from any subsequent hillslopes.

HESSD
12, 8175–8220, 2015

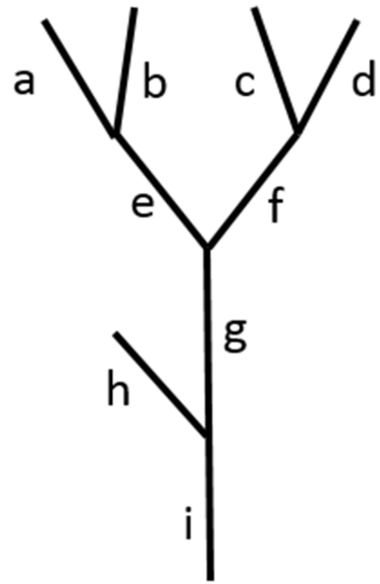

Figure 3. A small sample network to describe how total streamflow is computed.

HESSD
12, 8175–8220, 2015

On the propagation of diel signals in river networks using analytic solutions

M. Fonley et al.

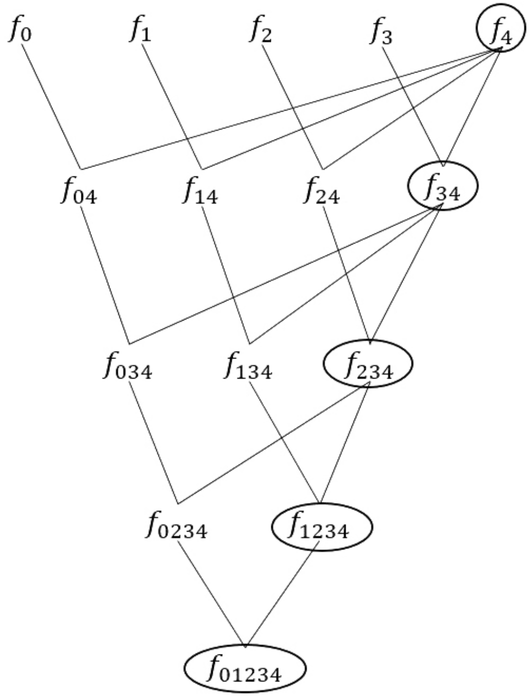

Figure 4. A visual representation of the computation of $\mathcal{F}_{jn}$ for the case $n = 4$.

HESSD
12, 8175–8220, 2015

On the propagation of diel signals in river networks using analytic solutions

M. Fonley et al.

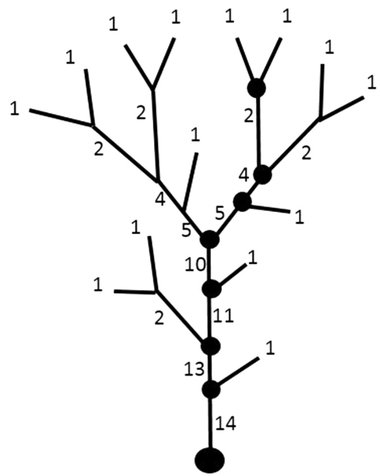

Figure 5. The Mandelbrot-Viscek tree of magnitude 14. The magnitude of each link is written next to the link. One link of each magnitude is distinguished by the dots along the network.

HESSD
12, 8175–8220, 2015

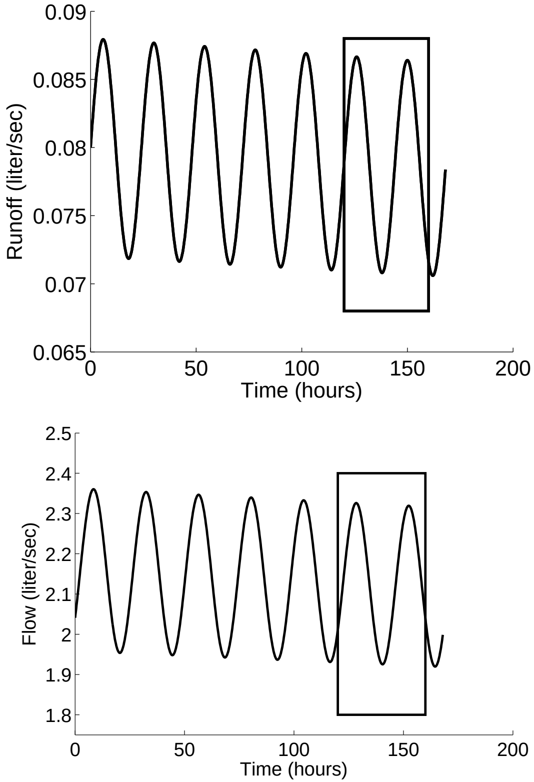

Figure 6. Sample runoff pattern (top panel) and resulting streamflow solution at the outlet in the uniform case (bottom panel) for $k = \frac{v}{l}$. To examine the oscillations more closely for different velocities, we will focus on a small section of the solution (highlighted by a box in each panel).

HESSD
12, 8175–8220, 2015

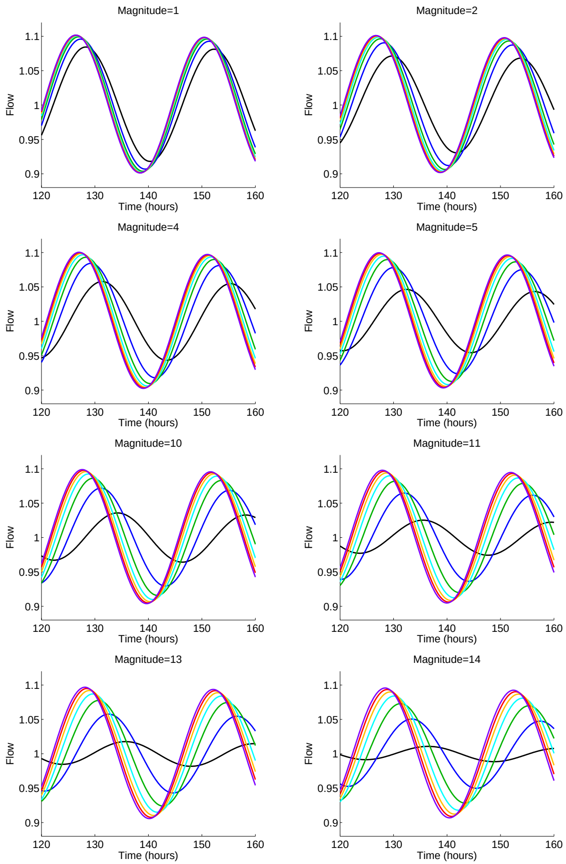

Figure 7. Flows at the outlet of each magnitude link using different k in each river simulation. The k values (with units of $[h^{-1}]$) are [0.38, 0.7, 1.02, 1.34, 1.66, 1.98, and 2.30] and are colored [black, blue, green, cyan, orange, red, and purple], respectively. The flows are normalized about the average flow.

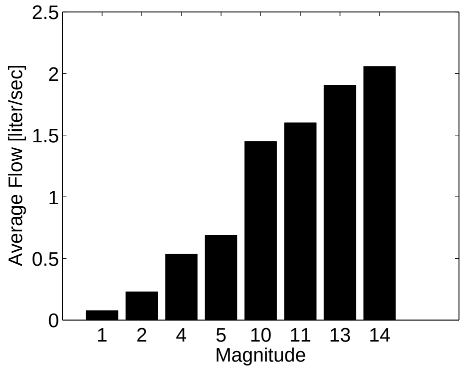

Figure 8. Average flows at different locations along the Mandelbrot–Viscek tree.

HESSD
12, 8175–8220, 2015

On the propagation of diel signals in river networks using analytic solutions

M. Fonley et al.

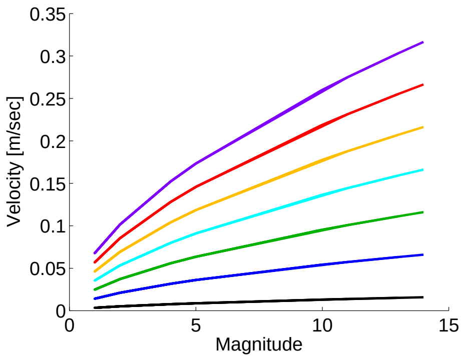

Figure 9. The velocity of each river link depends logarithmically upon the magnitude of the link. The maximum velocities applied are [0.016, 0.066, 0.12, 0.17, 0.22, 0.27, and 0.32] [$\mathrm{m\,s^{-1}}$] with the corresponding colors [black, blue, green, cyan, orange, red, and purple].

HESSD
12, 8175–8220, 2015

On the propagation of diel signals in river networks using analytic solutions

M. Fonley et al.

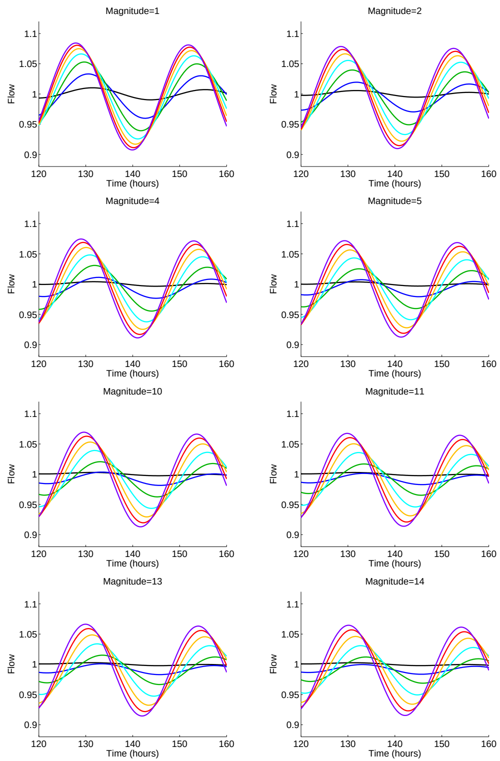

Figure 10. Flows at the outlet of each magnitude link using a different maximum velocity in the river network. Each link of the network has a different velocity and, thus, a different k value. The maximum velocity values are [0.016, 0.066, 0.12, 0.17, 0.22, 0.27, and 0.32], and they have corresponding k values (with units of [h^{-1}]) of [0.11, 0.47, 0.84, 1.20, 1.56, 1.92, and 2.28]. They are colored [black, blue, green, cyan, orange, red, and purple], respectively. The flows are normalized about the average flow.

HESSD
12, 8175–8220, 2015

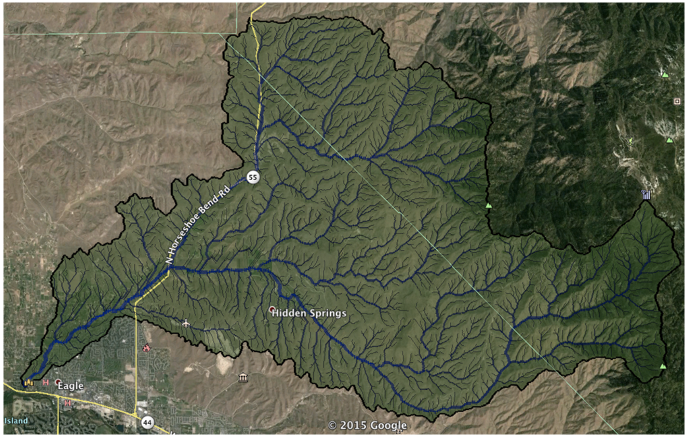

Figure 11. The Dry Creek watershed in Idaho.

HESSD
12, 8175–8220, 2015

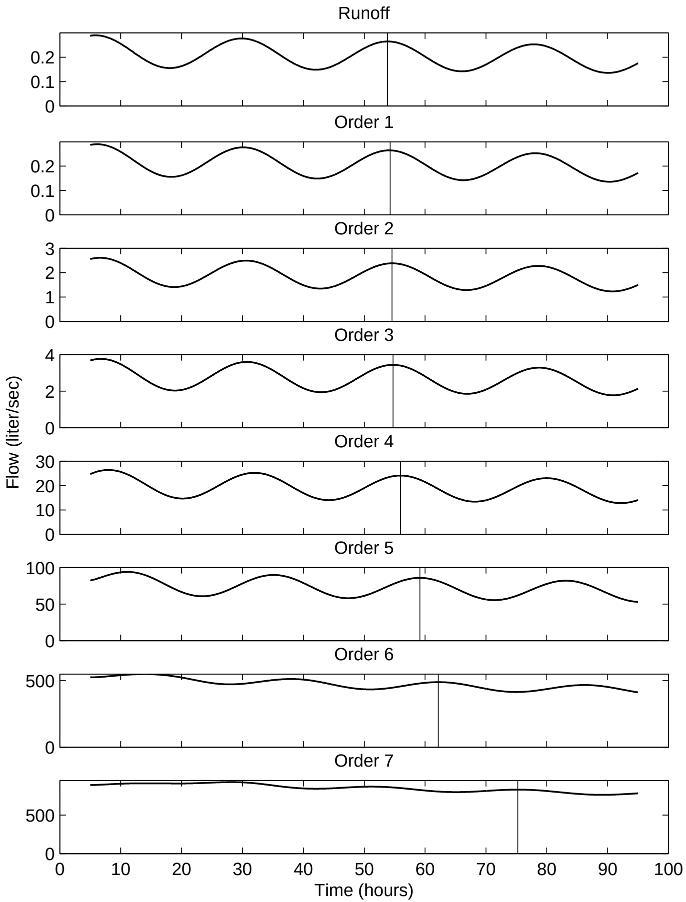

Figure 12. Runoff (top panel) and subsequent flows exiting links of different orders along the Dry Creek watershed. The vertical line in each panel highlights the time to a corresponding peak.

HESSD
12, 8175–8220, 2015

On the propagation of diel signals in river networks using analytic solutions

M. Fonley et al.